Jordan Journal of Civil Engineering, Volume **17**, No. **4**, **2023**
DOI: https://doi.org/10.14525/JJCE.v17i4.04

Three-dimensional Finite-element Analysis of the Influence of Tunneling on Pile Foundations

Moamen Abd El Raouf [1)*] ***and Khaled M. M. Bahloul*** [2)]

[1)] Civil Engineering Department, Faculty of Engineering, Al-Azhar University, Qena, Egypt.
* Corresponding Author. E-Mail: moamenabdelmontaleb@azhar.edu.eg
[2)] Lecturer, Department of Construction Engineering, October High Institute of Engineering and Technology, Egypt.

ABSTRACT

Advancing tunnel boring machine (TBM) during tunnel construction induces a surface settlement, affecting adjacent buildings and facilities. A three-dimensional finite-element model (Plaxis 3D) was used to simulate and analyze this process. A comparison between the numerical model and field measurements of the Greater Cairo Metro (Line 3) was made to validate the obtained results. A sensitivity analysis was conducted to determine how changes in some parameters, such as constitutive models, pile position relative to the tunnel axis and pile spacing, affect the results of the finite-element model. Three constitutive models: hardening soil small (HSS), hardening soil (HS) and the Mohr-Coulomb (MC) models, were used to evaluate the effect of the constitutive models on the results. From the numerical analysis, it is clear that the numerical results are in good agreement with field measurements. The results of the HSS model are more realistic and closer to field measurements than those of the HS and MC models. Furthermore, the effect of the tunnel construction on the settlement of adjacent piles is virtually null at a distance of 2 D (where D is the tunnel diameter). Finally, increasing the pile spacing decreases the effect of tunnel excavation on adjacent pile foundations.

KEYWORDS: Tunneling, Numerical models, Constitutive models, Pile foundation, Pile spacing.

INTRODUCTION

Tunnels are the optimal solution to traffic problems in crowded cities. Moreover, tunnels also reduce traffic noise and pollution. Many studies have been conducted on the subject of the ground movement caused by tunneling and its effect on adjacent structures (Peck, 1969; Reilly and New, 1982; Attewell et al., 1986; Mair et al., 1993; Klar et al., 2005; Vorster et al., 2005; Klar et al., 2008; Marshall et al., 2010; Marshall et al., 2012; Fethi, 2015; Qingming et al., 2022).

Many buildings in urban areas are constructed on piles. Sometimes, it is necessary to construct tunnels closely beneath piles. This process may affect the stability of the overlying structures, such as buildings, bridges and piled embankments. In addition, tunneling may reduce the pile capacity to the point of failure (Marshall et al., 2020). Furthermore, tunnel construction induces soil movement and stress relief. Therefore, the end bearing capacity and shaft resistance of piles may be diminished. Moreover, the existing piles are subjected to additional axial forces, bending moment, lateral forces, deflection and settlement (Soomro et al., 2018). Consequently, the designers must take into consideration the following two factors:

1) The serviceability of the structure (e.g. the piles do not move due to ground movement).
2) The additional bending moment and axial force caused by ground movement in piles (Francesco Basile, 2014).

The effect of tunneling on pile foundations has been studied by many researchers using field data, experimental work, numerical modeling and analytical analysis (Jacobsz et al., 2002; Jacobsz et al., 2004; Lee et al., 2005; Kitiyodom et al., 2005; Pang et al., 2006; Selemetas et al.,2006; Cheng et al., 2007; Shong-Loong Chen et al., 2016; Hui Hu et al., 2021).

Received on 28/1/2023.
Accepted for Publication on 29/6/2023.

Two methods (simplified and numerical methods) can be used to estimate the impact of the tunneling process on pile foundations. The simplified method consists of two stages: after computing the soil movement, the effect of soil movement on piles is evaluated. The numerical methods include soil, pile and tunnel excavation modeling (Francesco Basile, 2014).

To predict the displacement of soil caused by tunneling, the soil-structure interaction problem can be examined using the finite-element method. The finite-element analysis results depend primarily on the input parameters and the soil model.

Ayasrah et al. (2021) conducted a parametric analysis utilizing MIDAS GTS software, which included the influence of tunnel diameter, the impact of distance between piles and tunnel and the effect of tunnel depth using modified Mohr-Coulomb. It was found that the tunnel depth has a significant impact on piles. Moreover, the tunnel diameter has a notable effect on the behavior of piles and the distance between tunnels and piles has a considerable impact on the behavior of piles.

Soomro et al. (2018) conducted three-dimensional simulations to investigate the effect of tunnel construction on pile foundation response. A parametric study was carried out to examine the impact of the tunnel's relative depth on the behavior of piles.

Moreover, Loganathan et al. (2011) conducted a numerical simulation using the finite-element software FLAC3D to investigate the effect of tunneling on pile caps of various configurations and the influence of pile length on the behavior of piles.

Thus, it can be inferred that most of the studies focused on determining how tunnel construction would affect foundations. However, the main objective of the current analysis is to examine the effect of the tunneling progress (soil removal and lining installation) on pile foundations. Moreover, a sensitivity analysis was performed to determine how changes in some parameters, like constitutive models, pile position relative to the tunnel axis and pile spacing, influence the results of the finite-element model.

In this analysis, the response of pile foundations to tunneling was investigated using Plaxis 3D. In addition, the estimates of ground movement and pile response were performed. Furthermore, the Greater Cairo Metro (Line 3) field measurements were compared to the results of numerical model for validation.

Case Study

As a case study for this investigation, the pile foundations of the Garage El-Attaba building adjacent to the Greater Cairo Metro (Line 3) were considered. In recent decades, the Greater Cairo Metro is one of the most significant transportation projects in Egypt and Africa. In 1987, the first metro line was inaugurated. Greater Cairo is one of the most densely populated cities in the world and the Greater Cairo Metro has helped alleviate its traffic crises. Its construction uses a tunnel boring machine (TBM). On the other hand, Line 3 of this metro begins at Imbaba station and terminates at Cairo airport, with a 47.87-km longth. In 2011, the construction of the first phase of line 3 started from Imbaba station to El-Attaba station, with a length of 4.3 km. Over this distance, the tunnel passes adjacent to the foundation of the Garage El-Attaba building. The internal and external diameters of the tunnel are 8.35m and 9.15 m, respectively. (NAT, 2017).

The vertical displacement around the building was monitored during construction at certain points (SSP.B, SSP. C, SSP.D, SSP. E and SSP.F). Furthermore, the vertical displacement of the building was measured from July 2010 to August 2010 at the point (ERP), as shown in Figure (1) (NAT, 2010). In this analysis, the field settlement was used to validate the results obtained from a finite-element model.

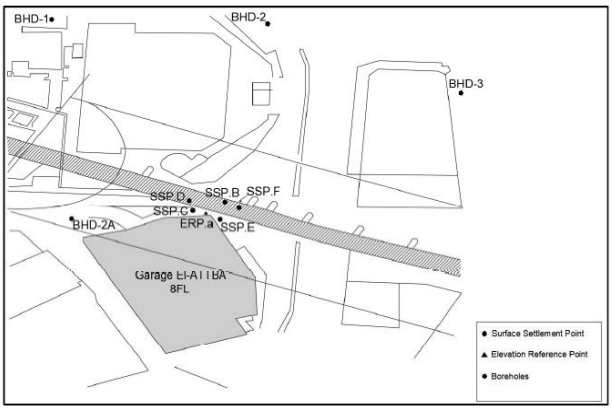

Figure (1): The layout of the monitoring system (after NAT, 2010)

Data of Garage El-Attaba Building

The dimensions of the Garage El-Attaba building are 77.04 m in length and 45.55 m in width. The building consists of eight stories and the nearest pile group is

located 6.45m from the tunnel's center, as shown in Figure (2). The building was supported by 245 bored concrete piles. With a diameter of 0.6m and a length of 20m, each pile has a bearing capacity of 120 tons. As presented in Figure (2), pile caps P1, P2, P3 and P4 are the closest pile caps to the tunnel axis and are considered the pile caps most affected by the tunnel construction. Therefore, only pile caps P1, P2, P3 and P4 were considered in this analysis. The details of pile caps are depicted in Figure (3).

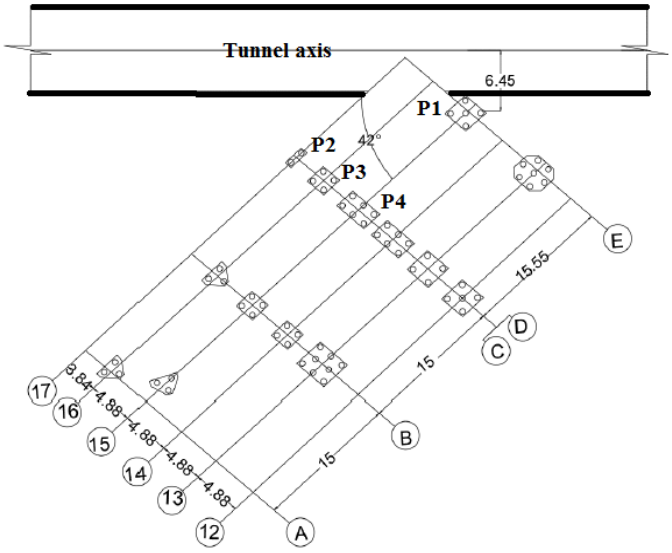

Figure (2): The location of the pile caps relative to the tunnel axis (all dimensions are in meters)

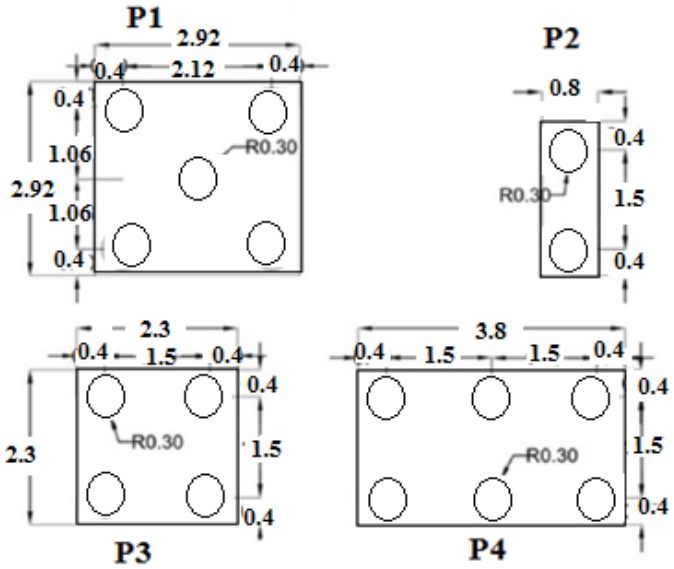

Figure (3): The details of pile caps (all dimensions are in meters) (after Mocarthy Brothers, 1984)

Soil Characteristics in the Study Area

Thirteen boreholes were drilled to investigate the soil conditions for line 3 of the Greater Cairo Metro. As shown in Figure (4), the soil profile beneath the Garage El-Attaba building consists of a 6.06 m-thick fill layer. The first layer is followed by a layer of silty clay with a thickness of 3.58 m. This layer is followed by a 13.81-m thick layer of upper sand that ranges from

medium to dense sand. In addition, a 1.15m-thick layer of sand and gravel appeared beneath the upper sand and a layer below the layer of sand and gravel is a stiff silty sand layer with a thickness of 1.38 m. Finally, there is a layer of dense sand called the lower sand that extends from the upper sand to the bedrock. The depth of the groundwater table varies between 2.0 m and 4.0 m from the ground surface (Hamza Associates, 2002).

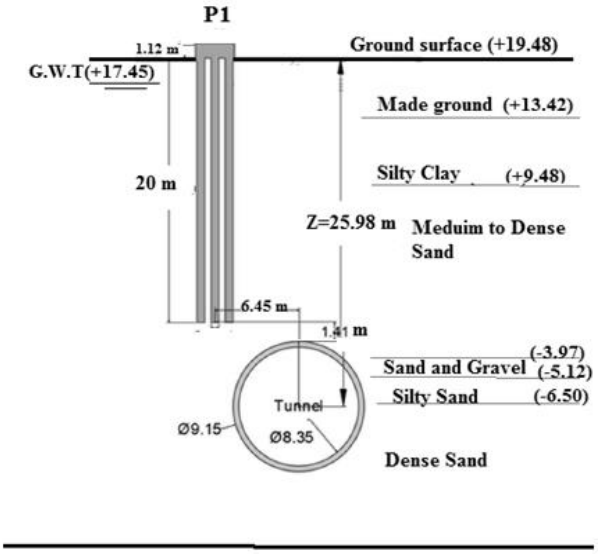

Figure (4): Soil profile in the study area and the position of the pile cap relative to the tunnel (after Hamza, 2002)

The Finite-element Model

The Plaxis 3D (ver. 22) computer program was used for conducting numerical analysis of geotechnical problems. This software is used to solve various geotechnical engineering problems, including the simulation of tunnel construction using a TBM (Tunnel Boring Machine). Default Plaxis Iterative Concurrent Solver, known as Picos (multicore iterative), was employed. Picos is a powerful iterative solver that effectively solves the system of equations in parallel on multicore processors. Typically, it is the quickest method to perform calculations (Bringreve et al., 2019).

The modeling of soil layers was done using the advanced HSS. The configuration of the numerical model is shown in Figure (5), where the dimensions of the model are 100 m in width, 100 m in length and 100 m in depth.

The distance from the lateral boundary of the model and the distance between the lower bound of the model from the top should be taken sufficient. So, the effects of the boundaries in the numerical model on the results were minimized. The displacement and the stress contours in the finite-element software indicate that this distance is sufficient (Maleki and Nabizadeh, 2021; Maleki et al., 2022; Maleki et al., 2023).

The 10-node tetrahedral elements' mesh used in the current analysis consists of 183547 nodes and 119078 elements. The mesh size used was a default medium mesh with automatic mesh refinement around the structural elements utilizing the enhanced mesh refinement feature in Plaxis 3D software (Bringreve et al., 2019; Maleki et al., 2019; Rahmani et al., 2022; Maleki and Imani, 2022).

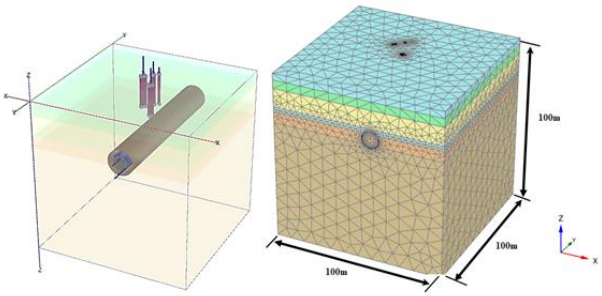

Figure (5): Numerical-model setup and 3D finite-element mesh

Modeling of the TBM shield and pile caps was conducted using plate elements. Piles are modeled using embedded beam elements, whereas the linear elastic model was used to simulate tunnel lining (Smulders et al., 2019).

To stimulate the soil-structure interaction, interface elements were applied. Moreover, the interface elements' decreased strength was applied using a strength-reduction factor (R_{inter}) equal to 0.8.

Table 1 presents the material properties of TBM shield pile caps, piles and tunnel lining (Mocarthy Brothers Company, 1984; NAT, 2010; Ayasrah et al., 2021).

Table 1. Properties of the structural elements used in the numerical analysis

Property	Pile Caps	Pile	TBM Shield	Tunnel Lining
Elasticity modulus E(MPa)	$3x10^4$	$3x10^4$	$2x10^5$	$1.4x10^4$
Unit weight γ (kN/m^3)	25	25	247	25
Poisson's ratio (υ)	0.15	0.15	0.1	0.1
Thickness (cm)	112	60	17	40

Hardening Soil Small-model Parameters

The HS-small model requires ten input parameters as follows:

- Three reference parameters of stiffness at reference stress level p^{ref} are required, which are: E_{50}^{ref} for triaxial compression, E_{oed}^{ref} for oedometer loading and E_{eur}^{ref}, which is unloading/reloading stiffness for triaxial compression.
- Unloading/reloading Poisson's ratio (υ_{ur}).
- Power (m) for stiffness depending on the stress level.
- Soil Shear strength parameters (ϕ, c andψ). (ϕ) friction angle, © cohesion and (ψ) dilation angle.
- Small shear strain modulus (G_o)
- The reference shear modulus at very small strains (G_o^{ref}) and shear strain ($\gamma_{0.7}$) at which $G_s = 0.722G_o$.

Small shear strain modulus (G_o) is calculated using Eq. (1).

$$G_o = G_o^{ref}\left(\frac{c\cos\varphi - \sigma_3'\sin\varphi}{c\cos\varphi + p^{ref}\sin\varphi}\right)^m \quad (1)$$

- The reference shear modulus at very small strains (G_o^{ref}) was estimated using Eq. (2) and shear strain ($\gamma_{0.7}$) at which $G_s = 0.722G_o$ using Eq. (3).

$$G_o^{ref} = 33 \times \frac{(2.97-e)^2}{1+e}\,(\text{MPa}) \quad (2)$$

$$\gamma_{0.7} \approx \frac{1}{9G_o}\{2c'[1+\cos(2\varphi')] - \sigma_1'(1+k_o)\sin(2\varphi')\} \quad (3)$$

where: σ_1= vertical principal effective stress, σ_3= horizontal, vertical effective stress, e = initial soil void ratio, k_o= coefficient of earth pressure at rest, c′= effective cohesion, φ′= effective angle of shearing resistance (Brinkgreve et al., 2019).

Table 2 shows the soil properties beneath Garage El-Attaba (Hamza Associates, 2002).

Table 2. Soil properties adopted in the finite-element method analysis

Parameter \ Soil	Made Ground	Silty Clay	Upper Sand	Sand and Gravel	Silty Sand	Lower Sand
Unit weight γ (kN/m^3)	17	19.5	19.5	20	19.5	19.5
Friction angle ϕ (Degree)	27	0	36	41	38	38
Cohesion (C) kPa	1	111	1	1	1	1
Dilatancy angle (ψ)	0	0	6	11	8	8
Poisson's ratio υ_{ur}	0.2	0.2	0.2	0.2	0.2	0.2
E_{50}^{ref} (MPa)	4	27	40	100	70	120
E_{oed}^{ref} (MPa)	4	27	40	100	70	120
E_{eur}^{ref} (MPa)	12	81	120	300	210	360
G_o^{ref} (MPa)	25	137.5	250	625	437.5	750
$\gamma_{0.7}$	$2x10^{-4}$	$2x10^{-4}$	$2x10^{-4}$	$2x10^{-4}$	$2x10^{-4}$	$2x10^{-4}$

Numerical Simulation of the Tunnel Construction

The tunnel construction process is performed by the tunnel boring machine (TBM), which is 9.0m long with a diameter of 9.15m.

Each subsequent phase will represent the tunnel advancement by 1.5m. The advancement rate of the

tunnel was 9.0 m per day.

To effectively simulate the tunnel construction, the following stages are implemented in the numerical-analysis program:

1- **Initial phase**: The generation of the initial stresses was performed using the K_0 procedure.
2- **Construction of piles and pile caps**: The construction of piles and pile caps was modeled by activating these structural elements.
3- **Applying building loading to pile caps**: This stage simulates the application of loads to the pile caps. The displacements were reset to zero to evaluate the impact of tunnel construction on the behaviour of piles and pile caps.
4- **Simulation of face excavation of the tunnel (step 1)**: In this stage, the simulation of excavation of the first 1.5m of the tunnel and application of face pressure (a bentonite pressure of the magnitude of 220 kPa), which is necessary for maintaining the excavation stability in front of the TBM machine.
5- **Simulation of advancement of TBM (steps 2 to 6):** In these steps, the simulation of TBM advancement is modeled by applying surface contraction.

The surface contraction is the application of linear surface contraction to simulate the cone part of the TBM shield, where the cross-sectional area of the tail of the TBM machine is 0.5%, which is smaller than the area in front of the TBM machine, as shown in Figure (6). Therefore, the reference contraction value (C_{ref}) = 0.5% with an increment $C_{inc,axial}$ (axial incremental contraction value) = -0.0667% was applied.

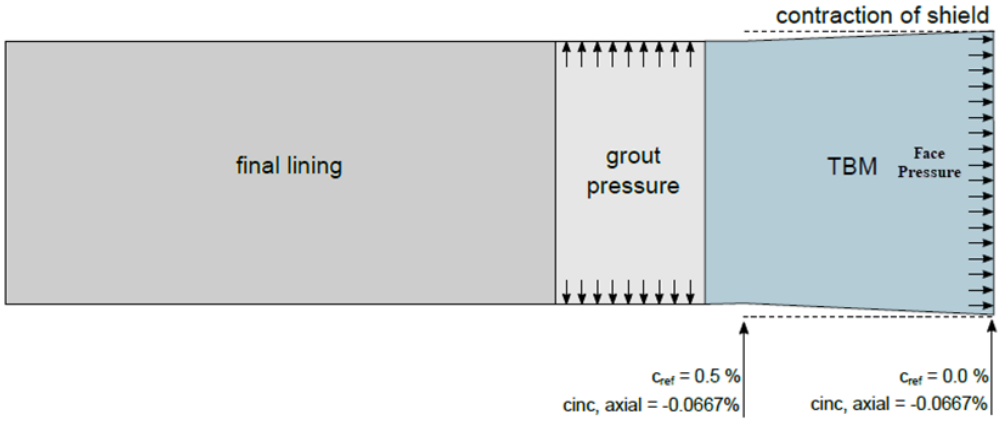

Figure (6): Schematic view of a TBM machine

6- **Simulation of applying grouting and jack thrusting (step 7):** In this step, the application of jack force is necessary to continue the tunneling process and grouting is modeled. This thrust, with a magnitude of 635 kPa, is applied to the tail of the TBM machine.
7- **Installation of the final lining ring (step 8)**: In this step, the installation of the lining ring or segment is simulated.
8- Stages (4-7) are repeated to simulate continued tunnel excavation until all tunnel segments are constructed.

Validation of the Finite-element Model

As mentioned earlier, the surface settlement at specific points around the building was monitored during construction. Therefore, field measurement of the ground settlement at two points (SSP.B and SSP.F) was compared with the ground settlement obtained from Plaxis 3D to validate the numerical-model results, as shown in Figures (7) and (8). The comparison between the results indicated that the numerical results agree with the field measurements.

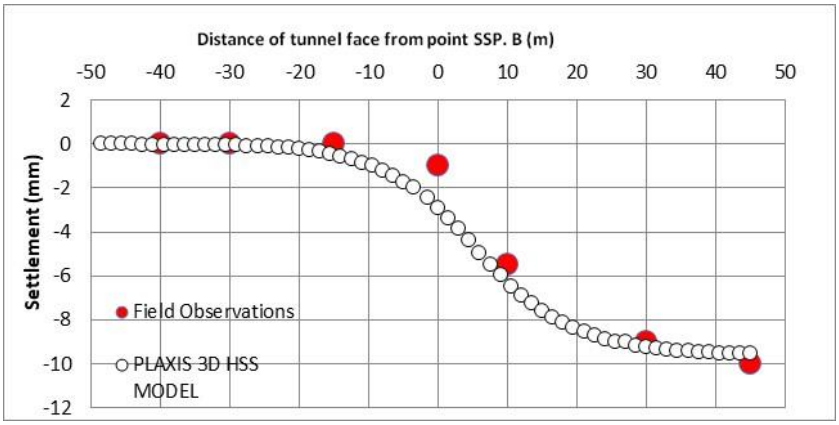

Figure (7): The ground settlement at the reference point (SSP.B) relative to the tunnel advancement

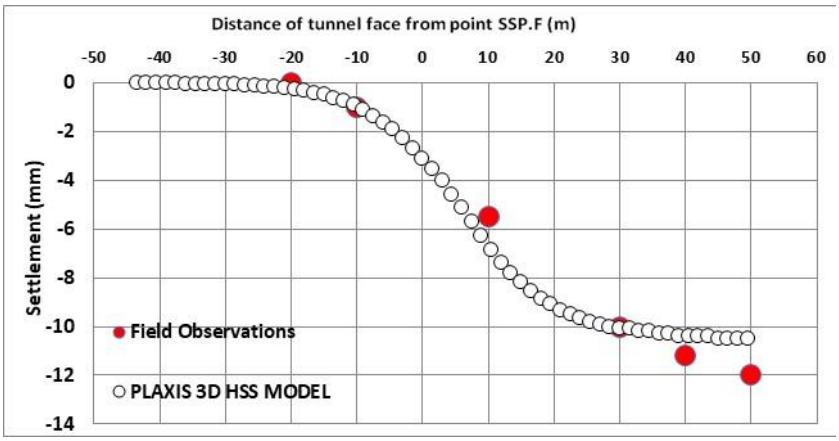

Figure (8): The ground settlement at the reference point (SSP.F) relative to tunnel advancement

Numerical-model Results

As shown in Figures (7) and (8), the maximum calculated settlement from the numerical analysis using the HSS model was 10 mm at a distance of 9.4D (D is the tunnel diameter) from the point (SSP.B). Moreover, the maximum settlement obtained from the numerical model was 10.5 mm at a distance of 9.4D from the point (SSP.F). Furthermore, the numerical results indicated that the ground settlement started to occur when the face of the TBM was at a distance of 2.2D from both points (SSP.B) and (SSP.F). Then, the settlement increased with the tunnel advancement.

The effects of the tunneling process on the bending moment, axial force and lateral defection for pile no. 1(the closest pile to the tunnel) were investigated.

Figure (9. a) shows the effect of tunnel construction on the lateral deflection for pile no. 1. The numerical results indicated that a significant lateral deflection occurred along the pile after tunnel construction due to soil movement. The lateral deflection was 2.2 mm at the pile head. Then, the lateral deflection decreased to 0.6 mm at a depth of 10 d (d is the pile diameter). Subsequently, the lateral deflection increased with increasing depth. Moreover, the maximum lateral deflection occurred at the pile tip due to the proximity of the tunnel to the pile tip. In addition, the soil movement is significant at the bottom of the pile. Figure (9.b) shows the effect of tunnel construction on the bending moment for pile no. 1. The results reflected that the bending moment increased significantly after the tunnel construction due to soil movement and the maximum bending moment occurred at16-m depth.

Additionally, Figure (9.c) illustrates the axial force along pile no. 1 before and after tunnel construction. The numerical results reported that the axial force increased due to ground movement after tunnel construction. The axial force increased at the pile head by about 13%. At a depth of 6.0 m, the axial force was equal before and after tunnel construction. Afterwards, the axial force decreased along the pile and the maximum axial force

occurred at the head of the pile.

According to the numerical-model results, the tunnel construction significantly affected the bending moments, axial forces and lateral displacement of the piles adjacent to the tunnel.

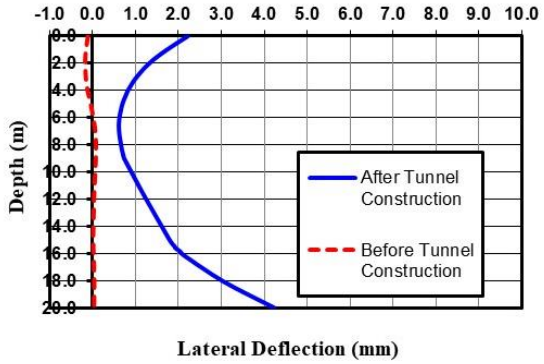

Figure (9) (a): Effect of the tunneling process on the pile lateral deflection

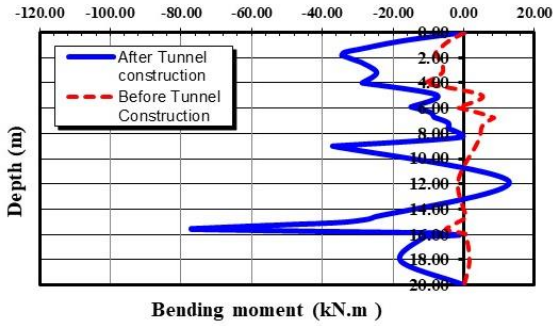

Figure (9) (b): Effect of the tunneling process on the pile bending moment

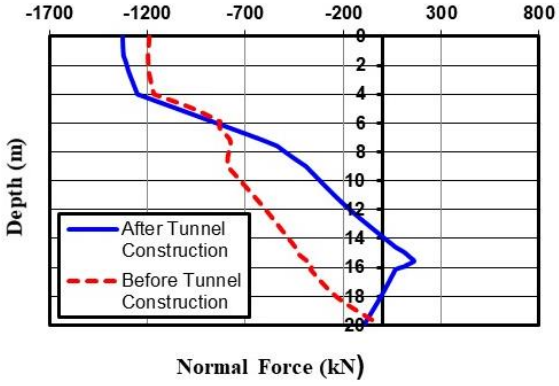

Figure (9) (c): Effect of the tunneling process on the pile axial force

Sensitivity Analysis

The sensitivity analysis of the numerical model was performed to determine how changes in some parameters affect the results of the finite-element model.

Constitutive Models

The constitutive model is an essential factor affecting the accuracy of the numerical-model results. Moreover, the mechanical properties of soil can be simulated and modeled *via* various constitutive models with different degrees of accuracy. Therefore, the Hardening Soil model with small strain (HSS), the Hardening Soil model (HS) and the Mohr-Coulomb model (MC) were adopted in this analysis to evaluate the effect of the constitutive models on the finite-element results. In the MC model, the strain was divided into plastic and elastic portions and the soil behavior followed Hooke's law. Hence, the failure contour is considered linear elastic and the accuracy of the model to simulate the deformation behavior of soil before failure occurs is limited (Brinkgreve, 2005).

In the HS model, the stress depends on the soil stiffness. The relation between the deviator stress and strain takes a hyperbolic shape. Moreover, the HS model contains advanced parameters, such as the reference stress for stiffness (P^{ref}), as the soil stiffness changes with the stress level. In the MC model, a constant value of the elasticity modulus is assumed. According to the previous considerations, the HS model is considered an advanced model in numerical analysis.

From Figures (10) and (11), it can be noticed that the maximum ground settlement analyzed *via* the MC model was 9.15 mm at a distance of 3.7D (D is the tunnel diameter) from the point (SSP.F). Additionally, the maximum ground settlement was 8.8 mm at a distance of 2.6D m from the point (SSP.B). When simulated using the HS model, the maximum ground settlement was 21.5 mm at a distance of 5.4D from the point (SSP.F). For the point (SSP.B), the maximum ground settlement was 20.4 mm at a distance of 4.9D. Moreover, the HSS model-based analysis indicated that the maximum ground settlement was 10.5 mm at a distance of4.9D from the point (SSP.F). For the point (SSP.B), the maximum ground settlement was 9.55 mm at a distance of 4.9D. According to the field observations, the maximum settlement was 12 mm at a distance of 5.4D from the point (SSP.F). For the point (SSP.B), the maximum ground settlement was 10 mm at a distance of 4.9D.

According to the information mentioned above, the analysis *via* the MC model gives the smallest value of ground settlement. Moreover, the analysis *via* the HS

model gives a higher value of ground settlement. Additionally, the results obtained from the modeling using the HSS model are more realistic and closer to field measurements than the results obtained from the analysis by the HS and MC models. This result is because when a very small strain is applied, the soil is considered elastic. Furthermore, soil stiffness decreases nonlinearly with increasing strain amplitude (Brinkgreve et al., 2012).

Furthermore, the HSS model is more accurate, because it considers more material parameters than the HS and MC models. The HSS model contains more parameters than the HS model. These parameters are the very-small-strain shear modulus (G_o), the shear strain ($\gamma_{0.7}$) where G_s (the secant shear modulus) = $0.7G_o$ and the reference shear modulus (G_o^{ref}) at a very small strain. The stiffness parameter G_o is an important parameter showing the initial part of the stress-strain curve (Atkinson and Sallfors, 1991). The additional parameters accurately describe the change of the soil stiffness with the strain, which reflects positively on the accuracy of the model results.

Accordingly, the HSS was selected in this analysis rather than the conventional MC and standard HS models, because the HSS model gives more accurate results, especially for simulating excavation problems like the case of tunneling construction.

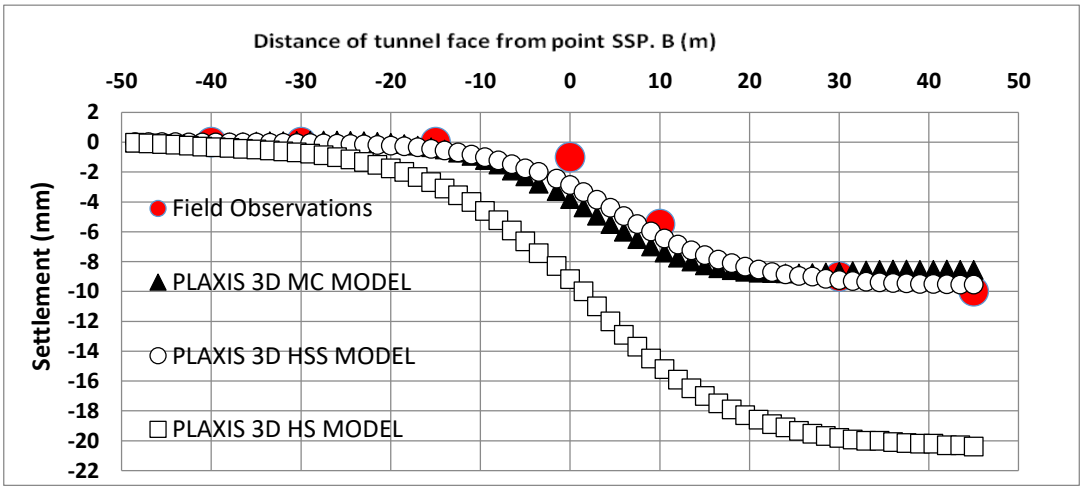

Figure (10): Effect of the constitutive models on the settlement at the reference point (SSP.B) relative to the tunnel advancement

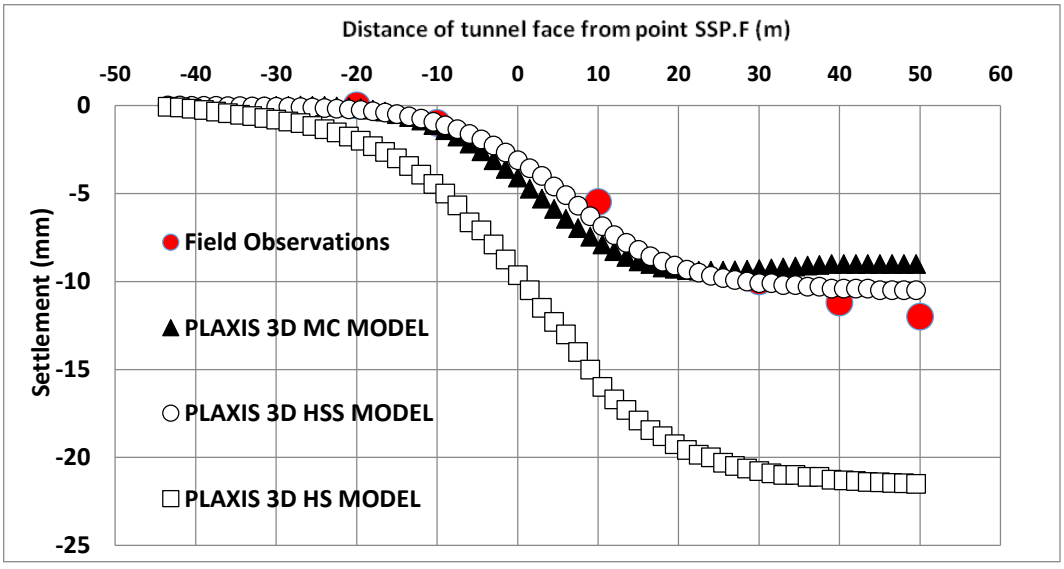

Figure (11): Effect of the constitutive models on the settlement at the reference point (SSP.F) relative to the tunnel advancement

Effect of Pile Position Relative to Tunnel Axis

This analysis investigated the effect of pile position relative to the tunnel axis. The distances between the axis of the tunnel and the center of the pile (X_P), as well as the pile settlement due to tunneling, were determined. Figure (12) shows that the pile closest to the tunnel (P_1) was the most affected pile by the construction of the tunnel. Moreover, the effect of the tunnel construction decreased by increasing the distance between the tunnel and the pile. When X_p=D (D is the tunnel diameter), the settlement decreased by about 50% from the maximum value. At X_p=1.5D, the settlement decreased by about 70% from the maximum value. Furthermore, the effect of the tunnel construction disappeared at a distance of 2D.

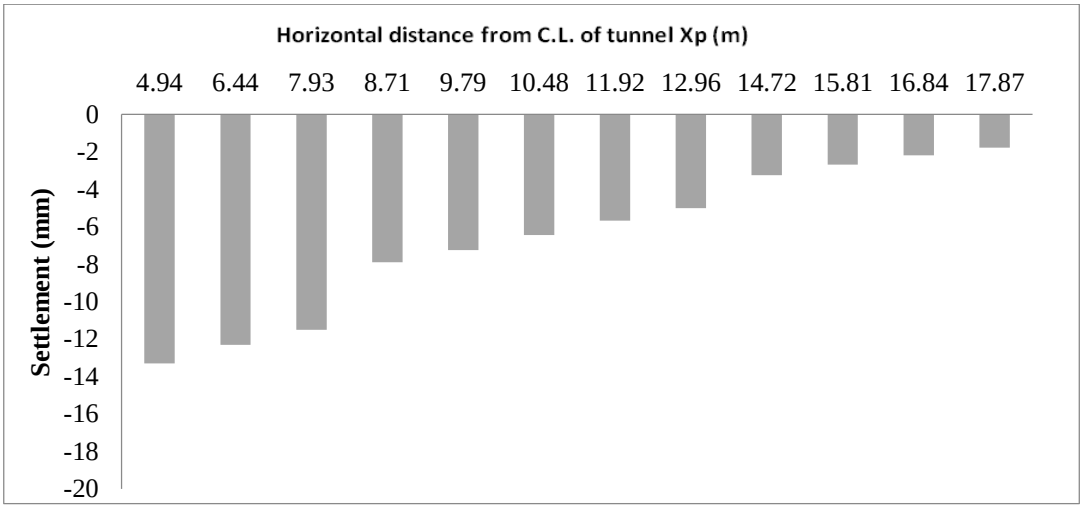

Figure (12): Effect of pile position relative to tunnel axis on vertical settlement

Effect of Pile Spacing

The building codes stipulate the minimum and maximum pile spacing. Generally, the pile spacing (S) may vary from 2d to 6d (d is the pile diameter). The pile spacing depends on many parameters, such as the soil characteristics and the type of piles (Murthy, 2003). The optimum spacing between piles to reduce the impact of the tunneling process on the adjacent piles was studied. The spacing between piles for Garage El-Attaba foundations is 1.5m. In this part, the pile spacing (S) was varied as follows: 2.5d, 3d and 3.5d. Then, the effects of tunnel construction on bending moment, axial force and lateral deflection were investigated for each pile spacing individually.

As shown in Figure (13a), the maximum bending moment occurred when (S=2.5d) at a depth of 27d, where the bending moment increased from 5.18 kN.m to 77.2 kN.m. Moreover, the maximum axial force at the pile head occurred at (S=2.5d), as shown in Figure (13b). It is worth noting that the axial force before the tunnel construction was compression. After the tunnel construction, a tension force was generated on the pile at a depth of 23d due to the ground movement. Furthermore, the axial force decreased as the pile spacing increased.

Figure (13c) reports that there is no noticeable change in the lateral deflection due to the difference in pile spacing. Moreover, the maximum lateral deflection at the pile head occurred at (S=3d) and the maximum lateral deflection at the pile tip occurred at (S=2.5d).

Figure (14) illustrates the effect of pile spacing on the vertical settlement. It can be seen that the vertical settlement decreases as the pile spacing increases.

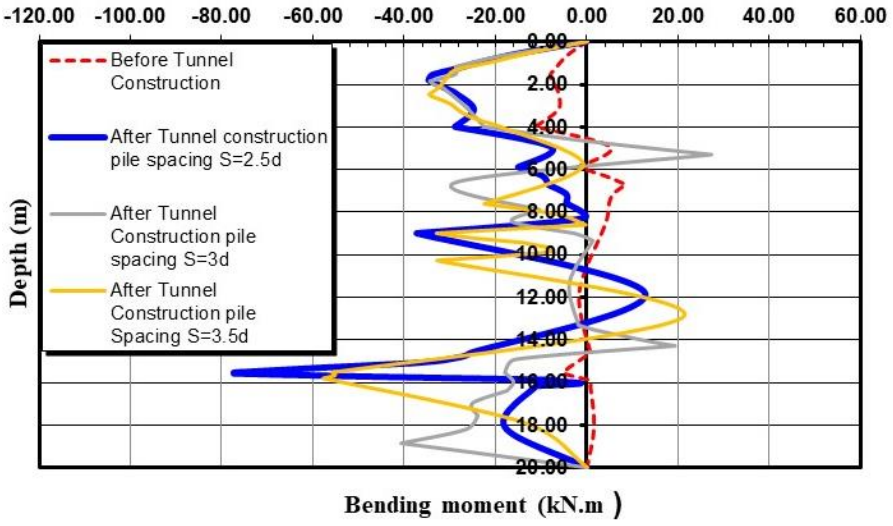

Figure (13) (a): Effect of pile spacing on bending moments

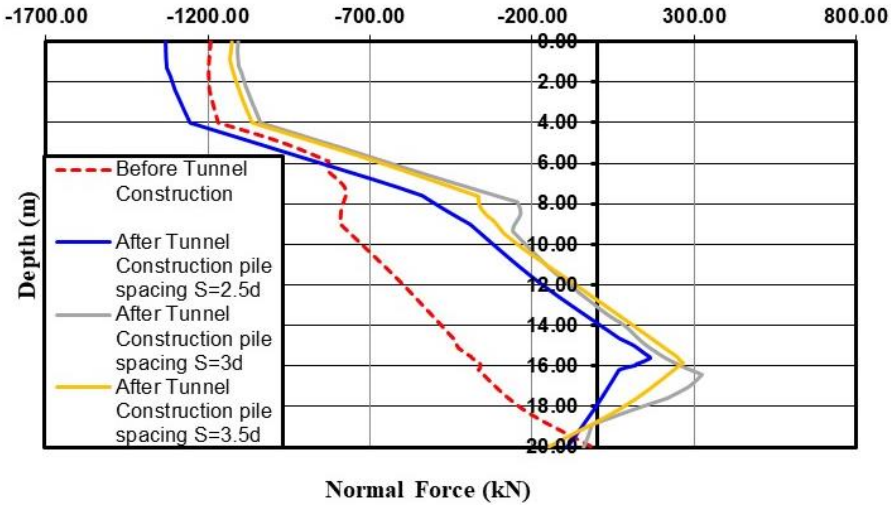

Figure (13) (b): Effect of pile spacing on axial force

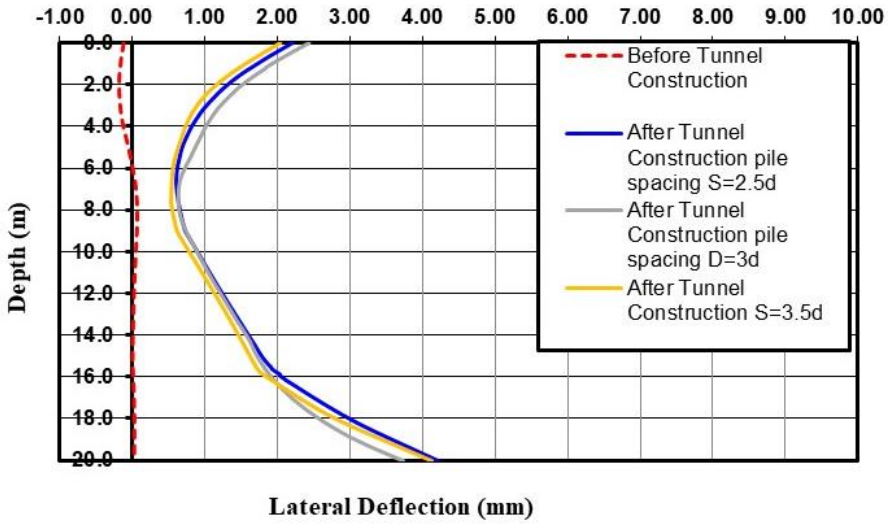

Figure (13) (c): Effect of pile spacing on lateral deflection

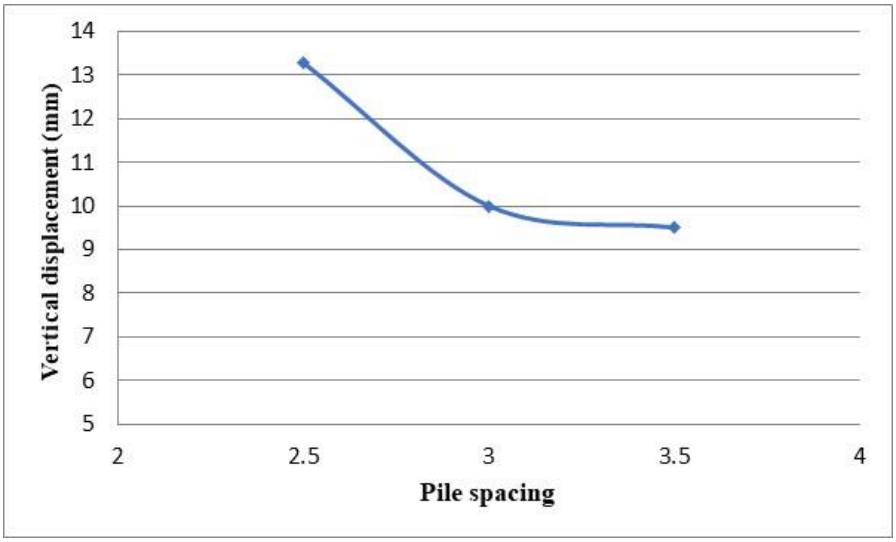

Figure (14): Effect of pile spacing on vertical displacement

The numerical-analysis results revealed that as the pile spacing increases, the impact of tunnel excavation on the piles decreases. This result can be considered when designing the pile foundations of the buildings that will be constructed near the tracks of the planned metro lines in the future, in order to reduce the impact of the tunneling process on the pile foundations.

The reason for this phenomenon is that in close piles, a highly compressed area of soil is generated between the piles due to the overlapping stresses, as shown in Figure (15). Therefore, when the soil moves due to the tunneling process, more soil disturbance occurs, especially in the compressed area of soil, which further affects the behavior of the piles. Moreover, in the case of closely spaced piles, the isobar extends to a greater distance.

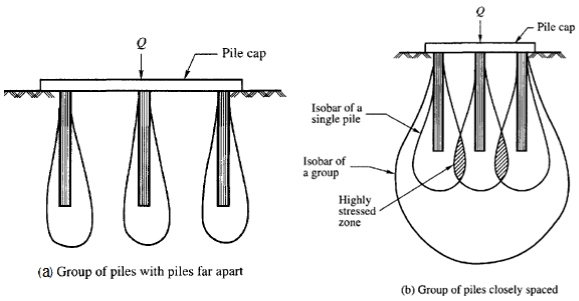

Figure (15): Pressure distribution of (a) closely spaced and (b) piles far apart (Murthy, 2003)

CONCLUSIONS AND RECOMMENDATIONS

Based on the analysis results, the following conclusions can be drawn:

1- Numerical results are in good agreement with field measurements.
2- The results obtained from the modeling by the HSS model are more realistic and closer to field measurement than the results obtained from the analysis by the HS and MC models.
3- The analysis *via* the MC model gives the least value of ground settlement. Moreover, the analysis *via* the HS model gives a higher value of ground settlement.
4- The effect of the tunnel construction on the settlement of adjacent piles nearly vanishes at a distance of 2D, where (D) is the tunnel diameter. Therefore, it is recommended that the distance between the tunnel and the adjacent piles should not be less than 2D.
5- It is recommended to increase the pile spacing to reduce the impact of tunnel excavation on adjacent pile foundations.

List of Symbols Used in the Study

Symbol	Definition
HSS	Hardening soil model with small strain
HS	Hardening soil model
MC	Mohr-Coulomb soil model
D	Tunnel diameter

d	Pile diameter
TBM	Tunnel boring machine
NAT	National Authority for Tunnels
R_{inter}	Strength-reduction factor
E	Modulus of elasticity
υ	Poisson's ratio
p^{ref}	Reference stress level
E_{50}^{ref}	Secant stiffness in standard drained triaxial test
E_{oed}^{ref}	Oedometer modulus
E_{eur}^{ref}	Unloading / reloading stiffness
υ_{ur}	Poisson's ratio for unloading - reloading
G_o^{ref}	Reference shear modulus at very small strains
G_o	Small-shear strain modulus
$\gamma_{0.7}$	Shear strain at which $G_s = 0.722G_o$
c	Soil cohesion
ϕ'	Effective angle of shearing resistance
σ_1	Major principal stress
$\sigma 3$	Minor principal stress
e_o	Initial soil void ratio
ko	Coefficient of earth pressure at rest
ψ	Dilatancy angle
C_{ref}	Reference contraction value
$C_{inc,axial}$	Axial incremental contraction value
X_p	Horizontal distance between the tunnel and the pile
S	Piles spacing.

REFERENCES

Atkinson, J.H., and Sallfors, G. (1991). "Experimental determination of soil properties". Proceedings of the 10th ECSMFE, 3, 915-956.

Attewell, P.B., Yeates, J., and Selby, A.R. (1986). "Soil movements induced by tunnelling and their effects on pipelines and structures". Blackie and Son, Ltd., UK.

Ayasrah, M., Qiu, H., and Zhang, X. (2021). "Influence of Cairo Metro tunnel excavation on pile deep foundation of the adjacent underground structures: Numerical study". Symmetry, 13 (2021), 426. https://doi.org/ 10.3390/sym13030426.

Brinkgreve, R.B.J. (2005). "Selection of soil models and parameters for geotechnical application". Proc. GeoFrontiers 2005: Soil Constitutive Models, Evaluation, Selection and Calibration, ASCE, Reston, VA, 69-97.

Brinkgreve, R.B.J. et al. (2012). "Plaxis 3D material models manual". Delft Univ. of Technology and Plaxis bv, Delft, Netherlands, 202.

Cheng, C.Y., Dasari, G.R., Chow, Y.K., and Leung, C.F. (2007). "Finite-element analysis of tunnel-soil-pile interaction using displacement controlled model". Tunn.Undergr. Space Technol., 22 (4), 450-466.

Fethi, K. (2015). "3D numerical study of tunnel advance core reinforcement: Application on tunnel T4 from the Algerian east-west highway". Jordan Journal of Civil Engineering, 9 (2), 139-149.

Francesco Basile. (2014). "Effects of tunnelling on pile foundations". Soils and Foundations, 54 (3), 280-295.

Hamza Associates. (2002). "Geotechnical investigation report (2002)". t; Hamza Associates: Cairo, Egypt.

Hui Hu, Yimo Zhu, Gang Zhang, Heng Zhang, and Peng Tu. (2021). "The environmental effects induced by a metro shield tunnel side-crossing on adjacent pile foundations and its impact partition". Advances in Civil Engineering, 2021, Article ID 8216724, 14 pages, 2021. https://doi.org/10.1155/2021/8216724

Jacobsz, S.W. (2002). "The effects of tunnelling on piled foundations".

Jacobsz, S.W., Standing, J.R., Mair, R.J., Hagiwara, T., and Sugiyama, T. (2004). "Centrifuge modeling of tunnelling near driven piles". Soils Found., 44 (1), 49-56.

Kitiyodom, P., Matsumoto, T., and Kawaguchi, K. (2005). "A simplified analysis method for piled raft foundations subjected to ground movements induced by tunneling". Int. J. Numer. Anal. Meth. Geomech., 29 (15), 1485-1507, ISSN 1096-9853.

Klar, A., Marshall, A.M., Soga, K., and Mair, R.J. (2008). "Tunneling effects on jointed pipelines". Can. Geotech. J., 45 (1), 131-139.

Klar, A., Vorster, T.E.B., Soga, K., and Mair, R.J. (2005). "Soil-pipe interaction due to tunnelling: Comparison between winkler and elastic continuum solutions". Geotechnique 55 (6), 461-466.

Lee, G.T.K., and Ng, C.W.W. (2005). "Effects of advancing open-face tunneling on an existing loaded pile". J. Geotech. Geoenviron. Eng., 131 (2), 193-201.

Loganathan, N., Poulos, H.G., and Xu, K.J. (2011). "Ground and pile-group responses due to tunneling". Soils Found., 41, 57-67.

Mair, R.J., Taylor, R.N., and Bracegirdle, A. (1993). "Subsurface settlement profiles above tunnels in clays". Geotechnique, 43 (2), 315-320.

Maleki, M., and Imani, M. (2022). "Active lateral pressure to rigid retaining walls in the presence of an adjacent rock mass". Arab J. Geosci., 15, 152. https://doi.org/10.1007/s12517-022-09454-z

Maleki, M., and Mir Mohammad Hosseini, S. (2019). "Seismic performance of deep excavations restrained by anchorage system using Quasi-static approach". Journal of Seismology and Earthquake Engineering, 21 (2), 11-21. https://doi.org/10.48303/jsee.2019.240810.

Maleki, M., and Mir Mohammad Hosseini, S.M. (2022). "Assessment of the pseudo-static seismic behavior in the soil nail walls using numerical analysis". Innov. Infrastruct. Solut., 7, 262. https://doi.org/10.1007/s41062-022-00861-5

Maleki, M., and Nabizadeh, A. (2021). "Seismic performance of deep excavation restrained by guardian truss structures system using quasi-static approach". SN Appl. Sci., 3, 417. https://doi.org/10.1007/s42452-021-04415-9.

Maleki, M., Khezri, A., Nosrati, M. et al. (2023). "Seismic amplification factor and dynamic response of soil-nailed walls". Model Earth Syst. Environ., 9, 1181-1198. https://doi.org/10.1007/s40808-022-01543

Marshall, A.M., Farrell, R.P., Klar, A., and Mair, R.J. (2012). "Tunnels in sands the effect of size, depth and volume loss on greenfield displacements". Geotechnique, 62 (5), 385-399.

Marshall, A.M., Franza, A., and Jacobsz, S.W. (2020). "Assessment of the post-tunneling safety factor of piles under drained soil conditions". J. Geotech. Geoenviron. Eng., 146 (9), 04020097. http://dx.doi.org/10.1061/(ASCE)GT.1943-5606.0002348.

Marshall, A.M., Klar, A., and Mair, R.J. (2010). "Tunneling beneath buried pipes: A view of soil strain and its effect on pipeline behavior". ASCE J. Geotech. Geoenviron. Eng., 136 (12), 1664-1672.

Mocarthy Brothers Company. (1984). "Division of design and management, consultant of Attaba parking garage". Mocarthy Brothers Company, Cairo, Egypt.

Murthy, V.N.S. (2003). "Geotechnical engineering: principles and practices of soil mechanics and foundation engineering". Marcel Dekker, Inc., New York.

NAT (National Authority for Tunnels). (2010). "Tunnel from Attaba to Geish Shaft monitoring measurements: Contract N 49/Metro, Phase 1". National Authority for Tunnels, Cairo, Egypt, 2010, 270-271.

NAT (National Authority for Tunnels). (2017). "Information of Greater Cairo metro line-3". Line-3, (Aug. 20, 2017).

Pang, C.H., Yong, K.Y., Chow, Y.K., and Wang, J. (2006). "The response of pile foundations subjected to shield tunneling". In: Bakker, K.J., Bezuijen, A., Broere, W. and Kwast, E.A. (Eds.), 5th International Symposium on Geotechnical Aspects of Underground Construction in Soft Ground. Taylor & Francis, 737-743, ISBN 978-0-415-39124-5.

Peck, R.B. (1969). "Deep excavations and tunnelling in soft ground". In: 7th International Conference on Soil Mechanics and Foundation Engineering, Mexico city, 225-290.

Qingming, J., Youqian, G., Xiaoshuang, L., and Xuansheng. (2022). "Construction settlement prediction of shield tunnel in soft-soil area". Jordan Journal of Civil Engineering, 16 (3), 2022.

Rahmani, F., Hosseini, S.M., Khezri, A. et al. (2022). "Effect of grid-form deep soil mixing on the liquefaction-induced foundation settlement, using numerical approach". Arab J. Geosci., 15, 1112. https://doi.org/10.1007/s12517-022-10340-x.

Reilly, O., and New M.P., B.M. (1982). "Settlements above tunnels in the United Kingdom: Their magnitude and prediction". In: Tunnelling 82, Papers Presented at the 3rd International Symposium, Inst. of Mining and Metallurgy, London, England, Brighton, England, 173-181.

Selemetas, D., Standing, J.R., and Mair, R.J. (2006). "The response of full-scale piles to tunnelling. In: Bakker, K.J., Bezuijen, A., Broere, W., and Kwast, E.A. (Eds.), 5th International Symposium on Geotechnical Aspects of Underground Construction in Soft Ground". Taylor & Francis, 763-769.

Shong-Loong Chen, Shen-Chung Lee, and Yu-Syuan Wei (2016). "Numerical analysis of ground-surface settlement induced by double-O tube shield tunneling". J. Perform. Constr. Facil., 30 (5), 04016012.

Smulders, C.M., Hosseini, S., and Brinkgreve, R. (2019). "Improved embedded beam with interaction sur-face". In: Sigursteinsson, H., Erlingsson, S., and Bessason, B. (Eds.) Proceedings of the 17th European Conference on Soil Mechanics and Geotechnical Engineering". COC, Reykjavík, Iceland, 1048-1055.

Soomro, M.A., Bangwar, D.K., and Keerio, M.A. (2018). "3D numerical analysis of the effects of an advancing tunnel on an existing loaded pile group". Eng. Technol. Appl. Sci. Res., 8 (1), 2520-2525, Feb. 2018.

Vorster, T.E.B., Klar, A., Soga, K., and Mair, R.J. (2005). "Estimating the effects of tunneling on existing pipelines". J. Geotechn. Geoenvironm. Eng., 131 (11), 1399-1410.